European Journal of Radiology 120 (2019) 108701

Contents lists available at ScienceDirect

European Journal of Radiology

journal homepage: www.elsevier.com/locate/ejrad

Research article

Breast cancer phenotype influences MRI response evaluation after neoadjuvant chemotherapy

Erika M.S. Negrão[a], Juliana A. Souza[b], Elvira F. Marques[b], Almir G.V. Bitencourt[b,*]

[a] Prevention Institute - Hospital de Câncer de Barretos, Campinas, SP, Brazil
[b] Imaging Department - A.C.Camargo Cancer Center, São Paulo, SP, Brazil

ARTICLE INFO

Keywords:
Magnetic resonance imaging
Neoadjuvant therapy
Pathological response
Triple negative radiological response
Her2
Breast neoplasms

ABSTRACT

Purpose: To evaluate which factors may influence magnetic resonance imaging (MRI) performance in the detection of pathologic complete response (pCR) after neoadjuvant chemotherapy (NAC).
Method: This retrospective study included 219 patients diagnosed with invasive breast carcinoma who underwent breast MRI before and after NAC. The MRI findings were compared to gold standard pathological examinations. Resolution of invasive breast disease was defined as pCR.
Results: The mean age of our cohort was 48 years (range: 20–85). The molecular subtypes included: Luminal B/Her-2 negative (n = 89; 40%), triple-negative (n = 69; 32%), Luminal B/Her-2 positive (n = 43; 20%), and Her-2 overexpression (n = 18; 8%). MRI analysis after NAC showed complete response in 76 cases (35%), while pathological analysis of surgical specimens after NAC detected pCR in 85 cases (39%). The accuracy of MRI in diagnosing pCR was 80%, with 69% sensitivity, 87% specificity, and positive and negative predictive values of 78% and 82%, respectively. The only factor statistically associated with a higher discordance rate between MRI and pathologic response was the presence of non-mass enhancement at pre-treatment MRI (p = 0.003).
Conclusions: MRI demonstrated good accuracy in predicting pCR after NAC among the breast cancer patients examined. However, non-mass enhancement at pre-treatment MRI negatively affected the diagnostic performance of MRI in assessing treatment response after NAC.

1. Introduction

Neoadjuvant chemotherapy (NAC) is the standard treatment for locally advanced breast cancer, and it is also widely applied to smaller tumors [1]. Several prospective, randomized studies have shown that preoperative therapy is equivalent to adjuvant chemotherapy in terms of patient survival and distant metastasis [2]. In addition, NAC allows more patients to receive conservative surgical treatment [3].

Magnetic resonance imaging (MRI) is an important tool to evaluate tumor extent and response to treatment. The ability of MRI to detect breast cancer and its varied morphologies has allowed this method to classify phenotype categories of breast cancer [4]. Furthermore, these phenotypes can be associated with response to chemotherapy and can provide an indication for conservative breast surgery [5,6]. MRI has been shown to be the most sensitive imaging modality for evaluating tumor response after NAC [7]. However, discrepancies between MRI findings and surgical pathology have been well documented. While overestimation of residual disease by MRI may result in more extensive surgery than is required, underestimation may result in insufficient surgery, leading to positive margins and additional operations [8].

Achievement of pathologic complete response (pCR) after NAC is associated with better prognosis in breast cancer patients, especially when more aggressive subtypes are present [9]. Breast MRI can accurately assess treatment response after NAC in most cases [8], however it is important to know when MRI may be less accurate. Despite many published articles have evaluated the accuracy of breast MRI after NAC, few papers have assessed what tumor characteristics could be related to radiologic-pathologic discordance in this setting [10–12]. Therefore, the objective of this study was to evaluate factors that may influence the performance of MRI in detecting pCR after NAC.

2. Methods

This observational, retrospective, and unicentric study was approved by the institutional Research Ethics Committee. A total of 219 patients were identified who were diagnosed with invasive breast carcinoma and underwent breast MRI before and after NAC between October 2014 and July 2017.

* Corresponding author at: Imaging Department - A.C.Camargo Cancer Center, R. Prof. Antonio Prudente, 211, São Paulo, SP, 09015-010, Brazil.
E-mail address: almir.bitencourt@accamargo.org.br (A.G.V. Bitencourt).

https://doi.org/10.1016/j.ejrad.2019.108701
Received 19 June 2019; Received in revised form 4 September 2019; Accepted 2 October 2019

2.1. MRI evaluations

MRI studies were conducted with a high-field system (1.5 T, Achieva, Philips Healthcare, Best, Netherlands) with a dedicated 8-channel breast coil. Images were obtained before and after administration of the paramagnetic contrast agent, gadopentetate dimeglumine (Gd-DTPA, 20 ml dose, 3 ml/s infusion rate). Prior to administration of Gd-DTPA, T1 gradient-echo phase, three dimensional (3D) imaging was acquired in the axial plane (TR/TE, 627/8.0 ms; 3 mm-thick slices; 280 × 399 matrix; FOV, 250 mm). A fat-saturated short tau inversion recovery (STIR) sequence in the sagittal plane of both breasts was also acquired (TR/TE, 5127/80 ms; 3 mm-thick slices; 220 × 208 matrix; FOV, 220 mm). Five gradient-echo phases in T1, 3D, and in the axial plane were further obtained by using fat suppression for dynamic examination (TR/TE, 5.1/2.5 ms; 1 mm-thick slices; 352 × 429 matrix; FOV, 300 mm). The first phase was obtained prior to the injection of contrast reagent, the second phase was obtained 20 s after the injection of contrast agent, and another phase was obtained in the subsequent minutes with a temporal resolution of 60–90 s. Pre-contrast images were subtracted from post-contrast images to provide better viewing of the highlighted areas. The last sequence consisted of a sagittal T1-weighted, 3D gradient-echo pulse sequence with fat signal suppression (TR/TE, 5.5/2.9 ms; 1 mm-thick slices; 368 × 364 matrix; FOV, 220 mm).

Breast lesions detected by MRI were classified according to the 5th edition Breast Imaging Reporting and Data System (BI-RADS®) lexicon [13] in mass, non-mass enhancement (NME), or both (mass and NME). The lesions were also classified as single or multiple (e.g., multicentric or multifocal disease, respectively), and their dimensions were classified according to TNM staging for breast cancer [14]. For post-treatment MRI, radiologic complete response (rCR) was defined as the absence of enhancement in the topography of the previous lesion or metallic clip, or when enhancement was equal to or lesser than the normal breast tissue, as previously described [15]. Breast MRI examinations after NAC were independently analyzed by two radiologists with 4-years and 10-years experience in breast imaging, respectively. In addition, both radiologists were blinded to the pathological results. Discordant cases achieved consensus with discussion and then were compared with pathological outcome (gold standard).

2.2. Pathological evaluation

All pre-treatment biopsies were reviewed by the institution's pathology department. Immunohistochemical data were used to classify breast carcinomas into five molecular subtypes: Luminal A (expression of estrogen/progesterone receptors and Ki-67 expression < 20%); Luminal B/Her-2 negative (positive for estrogen/progesterone receptors and Ki-67 expression ≥ 20%); Luminal B/Her-2 positive (positive for estrogen/progesterone receptors and Her-2 overexpressed); Her-2 overexpressed (negative hormone receptors expression and Her-2 overexpressed); or triple-negative (negative for both hormone receptors and Her-2).

Surgical treatment was performed at the same institution for all of the cases examined and the corresponding surgical specimens were evaluated according to Residual Cancer Burden (RCB) criteria for pathological response [16]. Resolution of invasive breast disease was defined as pCR, and cases of pCR could include an exclusive residual in situ component and exclusive axillary micrometastasis.

2.3. Statistical analysis

Statistical analyses were performed by using SPSS for Windows, version 20.0 (SPSS Inc., Chicago, IL, USA). Frequency analysis was performed to characterize the samples examined. Fleiss' Kappa coefficient (K) was used to assess interobserver agreement for the MRI response evaluations. Agreement was considered poor (K < 0.19), weak (0.20 < K > 0.39), moderate (0.40 < K > 0.59), substantial (0.60 < K > 0.79), or almost perfect (K > 0.80).

Breast MRI analysis after NAC provided classification of rCR versus non-rCR and was compared to pathological response (gold standard) data. In order to assess MRI accuracy to identify patients who achieve pCR after NAC, we considered rCR as the "positive" result for analysis. Thus, true-positive MRI cases successfully detected pCR, while true-negative cases successfully detected residual invasive breast carcinoma. False-positive cases were classified as rCR by MRI, yet contained residual invasive breast carcinoma according to pathological analysis. False-negative cases were classified as non-rCR by MRI and as pCR according to pathological analysis. Sensitivity was calculated based on the ratio of true-positive cases to all pCR cases. Specificity was calculated based on the ratio of true-negative cases to non-pCR cases. MRI accuracy and positive and negative predictive values were also calculated.

To evaluate factors which could influence MRI performance to detect pCR, MRI findings were classified as concordant or discordant according to pathological response. For this analysis, MRI phenotype was classified in two categories, one including tumors presenting as mass, and the other including tumors presenting as NME or both (mass and NME). Student's *t*-test (or non-parametric Mann-Whitney test, as indicated) was used to compare quantitative variables between two groups. The analysis of variance (ANOVA) test or non-parametric Kruskal-Wallis test were applied to compare data from three or more groups. The Pearson Chi-square test with Yates correction or Fisher's exact test were used to compare categorical variables. For multivariate analysis, binary logistic regression was performed, with MRI results (concordant or discordant) used as dependent variables. In the regression model, all variables with p < 0.10 in the univariate analysis were included as predictors. Odds ratio (OR) was also calculated. The level of significance was set at 5%.

3. Results

The patients selected for this study had a mean age of 48 ± 10.7 years (range: 20–85). The predominant molecular subtype was Luminal B/Her-2 negative (n = 89; 40%), followed by triple-negative (n = 69; 32%), Luminal B/Her-2 positive (n = 43; 20%), and Her-2 overexpression (n = 18; 8%). In the pre-treatment MRI analysis, masses were detected in 149 cases (68%), NME was observed in 27 cases (12%), and both findings were observed in 43 exams (20%). Single lesions were observed in 137 cases (63%) and multifocal/multicentric lesions observed in 82 cases (37%). Mass lesions were less common among the Luminal subtypes (Fig. 1). According to TNM staging [14], 19 cases were classified as T1 (9%), 139 cases were classified as T2 (63%), and 61 cases (28%) were classified as T3.

MRI analysis after NAC showed rCR in 76 cases (35%). The

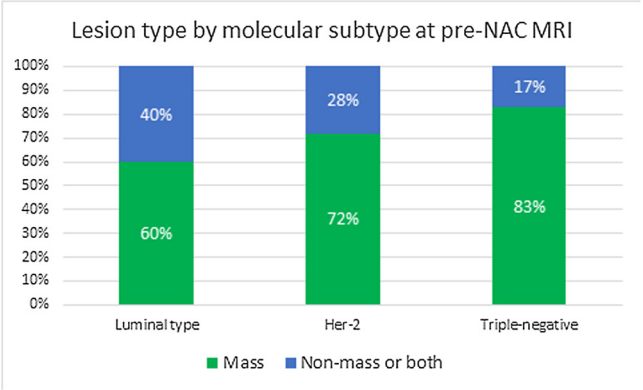

Fig. 1. Type of lesion found in pre-neoadjuvant chemotherapy MRI according to molecular subtype.

remaining 143 cases (65%) showed residual disease, including 43 masses (30%) and 100 cases (70%) of NME or both findings. A total of 119 (83%) single lesions and 24 (17%) multifocal or multicentric lesions were also detected after NAC. According to TNM staging, 90 cases (63%) were classified as T1, 40 cases (28%) were classified as T2, and 13 cases (9%) were classified as T3.

The overall agreement rate among the observers for residual breast lesions was substantial (k = 0.746). Moreover, the overall agreement rate was higher in the Luminal B/Her-2 negative subtype (k = 0.840) compared to Luminal B/Her-2 positive (k = 0.664), Her-2 overexpression (k = 0.658), and triple-negative (k = 0.679) subtypes.

Pathological analyses of surgical specimens collected after NAC indicated residual invasive breast carcinoma in 134 cases (61%) and pCR in 85 cases (39%). In addition, there were nine cases of exclusive in situ residual disease (six of them were classified as non-rCR in MRI) and six cases of exclusive metastatic disease in the axillary lymph node (five of them were classified as rCR in MRI). Based on the present findings, MRI accuracy in diagnosing pCR was 80%, with 69% sensitivity, 87% specificity, and positive and negative predictive values of 78% and 82%, respectively. Sensitivity and specificity were found to vary according to molecular subtype (Table 1).

A comparison of radiological and pathological responses showed that only one factor was statistically associated with a higher discordance rate, the presence of NME at pre-treatment MRI (p = 0.003). Other factors were analyzed and these did not present statistical significance between concordant and discordant cases (Table 2). Furthermore, multivariate analysis confirmed the influence of NME at pre-treatment MRI on the performance of MRI after NAC (Table 3).

4. Discussion

The results of the present study demonstrate that MRI exhibited 80% accuracy in identifying pCR after NAC in our breast cancer cohort. According to molecular subtype, MRI sensitivity was higher for Her-2 overexpressed and triple-negative subtypes. Regarding factors that influenced MRI performance after NAC, only the presence of NME at pre-treatment MRI was associated with discordance between radiological and pathological response evaluations, with statistical significance.

In breast MRI, the interpretation of multiple imaging features is considered fundamental for obtaining a differential diagnosis [18,19]. The phenotypic appearance of breast lesions has been widely studied and it has facilitated the differentiation of benign versus malignant lesions [20], invasive versus in situ carcinomas [21], and molecular subtypes of breast cancer [22]. For example, an unifocal round or oval mass is more frequently observed in triple-negative tumors [22,23]. In the present study, different proportions of tumor phenotypes were observed at pre-treatment MRI. In addition, while a predominance of mass lesions was observed for all subtypes, the highest percentage of mass lesions was observed among the triple-negative tumors. Meanwhile, the highest proportion of NME cases was associated with the luminal subtypes.

Many authors have suggested that MRI performance after NAC is related to molecular subtype [24,25]. Consistent with the results of a previous study [26], the current findings demonstrate that MRI sensitivity in identifying pCR was lower in cases involving luminal subtypes. Furthermore, tumor phenotype at pre-treatment MRI was found to be related to post-treatment MRI accuracy. The results of other studies also support the finding that NME at pre-treatment MRI makes evaluations of residual disease more difficult at post-treatment MRI [10,27]. In contrast, well-defined masses show greater agreement between MRI and pathology, thereby yielding more reliable predictions of pCR after surgery [6]. In the current study, cases presenting mass lesions at pre-treatment MRI showed almost 86% concordance between imaging and pathological response evaluations performed after NAC. The most widely accepted explanation for this finding is that locally advanced malignancies which present as mass lesions often shrink in a concentric pattern to a smaller mass after treatment. In contrast, NME often decrease as a scattered pattern of disease which may extend throughout the original area of involvement. In addition, small foci are difficult to detect with MRI [28]. Thus, it is important to understand MRI results after NAC, especially in assessments of residual disease, in order to

Table 1
Sensitivity, specificity, PPV, NPV, and accuracy of MRI in predicting pCR according to molecular subtype.

Molecular Subtype	Sensitivity	Specificity	PPV	NPV	Accuracy
All subtypes	69%	87%	78%	82%	80%
Luminal B	46%	89%	43%	91%	83%
Luminal B / Her-2	72%	76%	68%	79%	74%
Her-2 overexpression	77%	100%	100%	62%	83%
Triple-negative	75%	87%	75%	87%	83%

Abbreviations; PPV: positive predictive value; PPN: negative predictive value; MRI: magnetic resonance imaging; Her-2: human epidermal growth factor receptor-2.

Table 2
Univariate analysis of concordant and discordant cases according to molecular subtype classifications, patient age, phenotype, and lesion dimensions at pre- and post-chemotherapy MRI.

Variables		Concordant	Discordant	p-value
Age	< 50 y	107 (79.3%)	28 (20.7%)	0.367
	≥ 50 y	69 (82.1%)	15 (17.9%)	
Phenotype at MRI	Mass	128 (85.9%)	21 (14.1%)	0.003
	Non-mass enhancement or both findings	48 (68.6%)	22 (31.4%)	
Number of lesions according to MRI	Single	114 (83.2%)	23 (16.8%)	0.117
	Multifocal/ multicentric	62 (75.6%)	20 (24.4%)	
Lesion size at MRI	T1	13 (68.4%)	6 (31.6%)	0.210
	T2	116 (83.5%)	23 (16.5%)	
	T3	47 (77%)	14 (23%)	
Abnormal axillary lymph nodes at MRI	Negative	51 (83.6%)	10 (16.4%)	0.292
	Positive	125 (79.1%)	33 (20.9%)	
Histologic grade	1	5 (71.4%)	2 (28.6%)	0.811
	2	77 (81.1%)	18 (18.9%)	
	3	82 (79.6%)	21 (20.4%)	
Nuclear grade	1 or 2	41 (78.8%)	11 (21.2%)	0.429
	3	129 (81.1%)	30 (18.9%)	
Estrogen receptor	Negative	77 (81.1%)	18 (18.9%)	0.481
	Positive	99 (79.8%)	25 (20.2%)	
Progesterone receptor	Negative	85 (79.4%)	22 (20.6%)	0.433
	Positive	91 (81.3%)	21 (18.8%)	
Her-2 receptor	Not overexpressed	129 (81.6%)	29 (18.4%)	0.278
	Overexpressed	47 (77.0%)	14 (23.0%)	
Ki-67 expression	High (≥ 20%)	156 (78.8%)	42 (21.2%)	0.054
	Low (< 20%)	20 (95.2%)	1 (4.8%)	
Molecular subtype	Luminal B	74 (83.1%)	15 (16.9%)	0.680
	Luminal B/Her-2	32 (74.4%)	11 (25.6%)	
	Her-2 overexpression	15 (83.3%)	3 (16.7%)	
	Triple-negative	55 (79.9%)	14 (20.3%)	

Abbreviations; MRI: magnetic resonance imaging; Her-2: human epidermal growth factor receptor-2.

Table 3
Logistic regression model to predict MRI results concordant with pathological evaluations after NAC.

Independent variables	B	SE	OR	p-value
Presence of non-mass enhancement at MRI	1.294	0.371	3.648	< 0.01
Ki-67 > 20%	−1.945	1.065	0.143	0.07

Abbreviations; MRI: magnetic resonance imaging; NAC: neoadjuvant chemotherapy; SE: standard error; OR: odds ratio.

provide appropriate surgical treatment [6]. Moreover, each breast cancer subtype requires a tailored treatment strategy. Therefore, image interpretation can potentially play a key role in providing more precise recommendations for individual patients. Moreover, the ability to determine tumor phenotype, as well as molecular subtype, prior to NAC can also facilitate the identification of patients who will exhibit a more effective treatment response.

In the present study, there was no statistically significant difference on MRI performance between different molecular subtypes or other histological features. The presence of NME on pretreatment MRI was the only factor significantly associated to increased radio-pathologic discordance after NAC. However, there are some methodological differences to other studies that showed similar findings. Ko et al. showed that tumors presenting as diffuse NME on pretreatment MRI have greater radio-pathologic discrepancies in tumor size, when compared to other MRI patterns used in that study (single circumscribed mass, multiple masses and focal NME) [10]. Choi et al. evaluated only patients with rCR after NAC and found that calcifications in mammography, multifocal/multicentric lesions, and NME in pretreatment MRI were related to the presence of residual disease at pathology [12]. Future studies should help to better understand the role of NME in the response evaluation after NAC.

There were limitations associated with the present study. First, this retrospective study was conducted at a single cancer center. Second, other imaging methods such as ultrasonography and mammography were not evaluated after NAC. Third, another features which could affect MRI accuracy, such as background parenchymal enhancement and menopausal status, were not evaluated. We also did not evaluate the pattern of shrinkage of the breast tumor after NAC. At last, different definitions of pCR may potentially have an influence on MRI results. RCB criteria was used in the present study to characterize pathologic response to NAC because it is the most used and standardized method, however its definition of pCR includes residual in situ carcinoma, which does not have an impact on survival rates but may affect MRI results. However, there was only a small number of cases with pCR and residual ductal carcinoma in situ in our sample. Recently, Santamaria et al. demonstrated that MRI has a high accuracy to identify pathologic response after NAC, regardless of the definition of pCR [29].

5. Conclusions

In conclusion, MRI demonstrated good accuracy in the prediction of pCR after NAC in our cohort of breast cancer patients. In contrast, the presence of NME at pre-treatment MRI negatively affected the diagnostic performance of MRI in assessing treatment response after NAC. To confirm these findings, multicenter studies with a greater number of cases are needed.

Funding

This research did not receive any specific grant from funding agencies in the public, commercial, or not-for-profit sectors.

Declaration of Competing Interest

On behalf of my co-authors, I declare that we have no conflicts of interest to disclose.

Acknowledgements

None.

References

[1] M. Kaufmann, G. von Minckwitz, H.D. Bear, et al., Recommendations from an international expert panel on the use of neoadjuvant (primary) systemic treatment of operable breast cancer: new perspectives 2006, Ann. Oncol. 18 (2007) 1927–1934.
[2] D. Mauri, N. Pavlidis, J.P.A. Ioannidis, Neoadjuvant versus adjuvant systemic treatment in breast cancer: a meta-analysis, JNCI J. Natl. Cancer Inst. 97 (2005) 188–194.
[3] A.M. Chen, F. Meric-Bernstam, K.K. Hunt, et al., Breast conservation after neoadjuvant chemotherapy: the M.D. Anderson Cancer center experience, J. Clin. Oncol. 22 (2004) 2303–2312.
[4] S. Schrading, C.K. Kuhl, Mammographic, US, and MR imaging phenotypes of familial breast Cancer, Radiology 246 (2008) 58–70.
[5] L. Esserman, E. Kaplan, S. Partridge, et al., MRI phenotype is associated with response to doxorubicin and cyclophosphamide neoadjuvant chemotherapy in stage III breast cancer, Ann. Surg. Oncol. 8 (2001) 549–559.
[6] R.A. Mukhtar, C. Yau, M. Rosen, V.J. Tandon, N. Hylton, L.J. Esserman, Clinically meaningful tumor reduction rates vary by prechemotherapy MRI phenotype and tumor subtype in the I-SPY 1 TRIAL (CALGB 150007/150012; ACRIN 6657), Ann. Surg. Oncol. 20 (2013) 3823–3830.
[7] V. Londero, M. Bazzocchi, C. Del Frate, et al., Locally advanced breast cancer: comparison of mammography, sonography and MR imaging in evaluation of residual disease in women receiving neoadjuvant chemotherapy, Eur. Radiol. 14 (2004).
[8] M.B.I. Lobbes, R. Prevos, M. Smidt, et al., The role of magnetic resonance imaging in assessing residual disease and pathologic complete response in breast cancer patients receiving neoadjuvant chemotherapy: a systematic review, Insights Imaging 2013 (2013) 163–175.
[9] P. Cortazar, L. Zhang, M. Untch, et al., Pathological complete response and long-term clinical benefit in breast cancer: the CTNeoBC pooled analysis, Lancet 384 (2014) 164–172.
[10] E.S. Ko, B.-K. Han, R.B. Kim, et al., Analysis of factors that influence the accuracy of magnetic resonance imaging for predicting response after neoadjuvant chemotherapy in locally advanced breast Cancer, Ann. Surg. Oncol. 20 (2013) 2562–2568.
[11] Y. Kim, S.H. Sim, B. Park, et al., Magnetic resonance imaging (MRI) assessment of residual breast Cancer After neoadjuvant chemotherapy: relevance to tumor subtypes and MRI interpretation threshold, Clin. Breast Cancer 18 (2018) 549–567.
[12] W.J. Choi, H.H. Kim, J.H. Cha, et al., Complete response on MR imaging after neoadjuvant chemotherapy inbreast cancer patients: factors of radiologic-pathologic discordance, Eur. J. Radiol. 118 (2019) 114–121.
[13] C. D'Orsi, E. Sickles, E. Mendelson, Morris E. ACR BI-RADS Atlas, Breast Imaging Reporting and Data System, 5th ed., (2013) Virginia: Reston.
[14] S.R. Lakhani, I.O. Ellis, S.J. Schnitt, Tan P.H. van de VM, WHO Classification of Tumours of the Breast, 4th ed., IARC WHO Classification of Tumours, 2012.
[15] M.L. Marinovich, N. Houssami, P. Macaskill, et al., Meta-analysis of magnetic resonance imaging in detecting residual breast Cancer After neoadjuvant therapy, JNCI J Natl Cancer Inst. 105 (2013) 321–333.
[16] C.A.B.T. Osório, M.A. Chaves Júnior, F.A. Soares, Avaliação de resposta patológica em câncer de mama após quimioterapia neoadjuvante: padronização de protocolo adaptado, J. Bras. Patol. e Med. Lab. 48 (2012) 447–453.
[18] C. Kuhl, The current status of breast MR imaging part I. Choice of technique, image interpretation, diagnostic accuracy, and transfer to clinical practice, Radiology 244 (2007) 356–378.
[19] M. Goto, H. Ito, K. Akazawa, et al., Diagnosis of breast tumors by contrast-enhanced MR imaging: comparison between the diagnostic performance of dynamic enhancement patterns and morphologic features, J. Magn. Reson. Imaging 25 (2007) 104–112.
[20] S.A. Jansen, A. Shimauchi, L. Zak, X. Fan, G.S. Karczmar, G.M. Newstead, The diverse pathology and kinetics of mass, nonmass, and focus enhancement on MR imaging of the breast, J. Magn. Reson. Imaging 33 (2011) 1382–1389.
[21] M. Tozaki, K. Fukuda, High-spatial-resolution MRI of non-masslike breast lesions: interpretation model based on BI-RADS MRI descriptors, AJR Am. J. Roentgenol. 187 (2006) 330–337, https://doi.org/10.2214/ajr.187.3.w330.
[22] L.K.L. França, A.G.V. Bitencourt, H.L.S. Paiva, et al., Role of magnetic resonance imaging in the planning of breast cancer treatment strategies: comparison with conventional imaging techniques, Radiol. Bras. 50 (2017) 76–81.
[23] T. Uematsu, M. Kasami, S. Yuen, Triple-negative breast Cancer: correlation between MR imaging and pathologic Findings1, Radiology 250 (2009) 638–647.
[24] C.E. Loo, M.E. Straver, S. Rodenhuis, et al., Magnetic resonance imaging response monitoring of breast cancer during neoadjuvant chemotherapy: relevance of Breast Cancer subtype, J. Clin. Oncol. 29 (2011) 660–666.
[25] Y. Hayashi, H. Takei, S. Nozu, et al., Analysis of complete response by MRI following neoadjuvant chemotherapy predicts pathological tumor responses differently for molecular subtypes of breast cancer, Oncol. Lett. 5 (2012) 83–89.
[26] K.P. McGuire, J. Toro-Burguete, H. Dang, et al., MRI Staging After Neoadjuvant Chemotherapy for Breast Cancer: Does Tumor Biology Affect Accuracy? Ann. Surg. Oncol. 18 (2011) 3149–3154.
[27] S. Bahri, J.-H. Chen, R.S. Mehta, et al., Residual breast Cancer Diagnosed by MRI in patients receiving neoadjuvant chemotherapy with and without bevacizumab, Ann. Surg. Oncol. 16 (2009) 1619–1628.
[28] E.R. Price, J. Wong, R. Mukhtar, N. Hylton, L.J. Esserman, How to use magnetic resonance imaging following neoadjuvant chemotherapy in locally advanced breast cancer, World J. Clin. Cases 3 (2015) 607.
[29] G. Santamaria, X. Bargallo, S. Ganau, et al., Multiparametric MR imaging to assess response following neoadjuvant systemic treatment in various breast cancer subtypes: comparison between different definitions of pathologic complete response, Eur. J. Radiol. 117 (2019) 132–139.